

EFFECT OF DISCRETE HEATER AT THE VERTICAL WALL OF THE CAVITY OVER THE HEAT TRANSFER AND ENTROPY GENERATION USING LATTICE BOLZMANN METHOD

by

Mojtaba AGHAJANI DELAVAR, Mousa FARHADI^{*}, Kurosh SEDIGHI

Babol University of Technology, Faculty of Mechanical Engineering, Babol, Iran

Original scientific paper

UDC: 536.251/.253:519.876/.5

DOI: 10.2298/TSCI1102423A

In this paper lattice Boltzmann method was employed for investigation the effect of the heater location on flow pattern, heat transfer and entropy generation in a cavity. A 2-D thermal lattice Boltzmann model with 9 velocities, D2Q9, is used to solve the thermal flow problem. The simulations were performed for Rayleigh numbers from 10^3 to 10^6 at $Pr = 0.71$. The study was carried out for heater length of 0.4 side wall length which is located at the right side wall. Results are presented in the form of streamlines, temperature contours, Nusselt number, and entropy generation curves. Results show that the location of heater has a great effect on the flow pattern and temperature fields in the enclosure and subsequently on entropy generation. The dimensionless entropy generation decreases at high Rayleigh number for all heater positions. The ratio of averaged Nusselt number and dimensionless entropy generation for heater located on vertical and horizontal walls was calculated. Results show that higher heat transfer was observed from the cold walls when the heater located on vertical wall. On the other hand, heat transfer increases from the heater surface when it is located on the horizontal wall.

Key words: *natural convection, cavity, entropy generation, lattice Boltzmann method*

Introduction

The phenomenon of natural convection in enclosures has received considerable attention due to its importance in many applications, such as solar collectors, electronic cooling devices, building engineering, heat transfer through double glazing windows, geophysical applications, *etc.* Natural convection in enclosures can be historically classified in three groups: enclosure heated from below and cooled from above (Rayleigh–Benard problem), differentially heated enclosures, and enclosures with cross thermal boundary conditions. Several works about natural convection in many different areas are available, with experimental and numerical approaches. Chu *et al.* [1] investigated the effects of localized heating in rectangular channels. A numerical study was carried out by Refai *et al.* [2, 3] to investigate the influence of discrete heat sources on natural convection heat transfer in a

^{*} Corresponding author; e-mail: mfarhadi@nit.ac.ir

square enclosure filled with air. Nelson *et al.* [4] experimentally investigated the natural convection and thermal stratification in chilled-water storage systems. An experimental study of low-level turbulence natural convection in an air filled vertical square cavity was conducted by Ampofo *et al.* [5]. Adeyinka *et al.* in their work developed an uncertainty analysis for a newly measured variable of local entropy production [6]. Entropy production was measured with post-processing and spatial differencing of measured velocities from particle image velocimetry, as well as temperatures obtained from planar laser induced fluorescence. Poujol [7] experimentally and numerically investigated the transient natural convection in a square cavity heated with a time-dependent heat flux on one vertical. Oliveski *et al.* [8] analyzed numerically and experimentally the velocity and temperature fields at natural convection inside a storage tank. A finite element method was used to investigate the steady laminar natural convection flow in a square cavity with uniformly and non-uniformly heated bottom wall, and adiabatic top with cold vertical walls [9]. The effects of different Prandtl and Rayleigh numbers were investigated based on comprehensive analysis of heat flow pattern using Bejan's heatlines concept [10]. Beya *et al.* [11] investigated numerically the natural convection flow in 3-D tilted cubic enclosure at angle with respect to the vertical position. The enclosure was heated and cooled from the two opposite walls while the remaining walls were adiabatic.

The lattice Boltzmann method (LBM) is a powerful numerical technique based on kinetic theory for modeling the fluid flows and physics in fluids [12-16]. In the last decade the LBM has evolved as a significant success alternative numerical approach for the solution of a large class of problems. The advantages of LBM, in comparison with the conventional computational fluid dynamics (CFD) methods, include simple calculation procedure, easy and robust handling of complex geometries, simple and efficient implementation for parallel computation, and others [12, 16, and 17]. Several natural convection, 2-D and 3-D, problems have been simulated successfully with the different thermal lattice Boltzmann models or other Boltzmann-based schemes [18-25].

Optimized design of heat systems can be obtained within minimizing of entropy generation. Decreasing of entropy generation in heat transfer systems will make great increase in their performance. This field was attending greatly at fields such as cross-flow heat exchangers, power plants, energy storage systems, and refrigeration usages. Entropy generation is associated with thermodynamic irreversibility which exists in all heat transfer processes. By design consideration, minimizing of the entropy generation was investigated on heat transfer and thermal analysis of thermodynamics second law. Notable researches have been done to investigate importance of entropy generation in thermal systems. The early works for optimization design with minimizing the entropy generation were done by Bejan [26-31].

Demirel *et al.* [32] investigated the entropy generation due of heat transfer and fluid friction in a duct with isotherm walls. They reported that minimizing entropy generation will give a criterion to system optimization, and also that entropy generation can be minimized with proper selection of operating conditions and design parameters. In the work of Sahin [33], a comparative study of entropy generation inside of ducts with different shapes and determination of optimum duct shape subjected to isothermal boundary condition was done. Narusawa [34] made an analytical and numerical analysis of the second law for flow and heat transfer in a rectangular duct. In a more recent study, Mahmud *et al.* [35, 36] applied the second law analysis to fundamental convective heat transfer problems for non-Newtonian fluid through a channel between two parallel plates. Aïboud-Saouli *et al.* [37] investigated

entropy generation in a laminar, conducting liquid flow inside a channel made of two parallel heated plates under the action of transverse magnetic field. They also examined the effect of viscous dissipation on velocity, temperature and entropy generation.

In the study of Delaver *et al.* [38], the LBM was employed to investigate the effect of the heater location on entropy generation, flow pattern, and heat transfer in a cavity numerically. The study was carried out for heater length of $0.4H$ which is located at the lower wall of the cavity. The simulations were performed for Rayleigh numbers from 10^3 to 10^6 at $Pr = 0.71$. Results showed that the location of heater and Rayleigh number have great effects on the flow pattern and temperature fields in the enclosure and subsequently on entropy generation.

In this study, the heater part is located at left side wall of the cavity. The effect of heater location and Rayleigh number on overall heat transfer inside a square enclosure was investigated. A 2-D thermal LBM with 9 velocities, D2Q9, is used to solve the thermal flow problem. The simulations in each configuration have been made for Rayleigh numbers changing from 10^3 to 10^6 . Then to optimize system thermodynamically, the second law analyze has been applied to models and entropy generation has been calculated for different models to obtain optimum model.

The lattice Boltzmann method

In this study, the D2Q9 model has been used (fig. 1). After introducing Bhatnagar-Gross-Krook approximation, the general form of lattice Boltzmann equation with external force can be written as [14, 22]:

$$f_k(\bar{x} + \bar{c}_k \Delta t, t + \Delta t) = f_k(\bar{x}, t) + \frac{\Delta t}{\tau} [f_k^{\text{eq}}(\bar{x}, t) - f_k(\bar{x}, t)] + \Delta t \bar{F}_k \quad (1)$$

where Δt denotes lattice time step, \bar{c}_k is the discrete lattice velocity in direction k , \bar{F}_k – the external force in direction of lattice velocity, τ denotes the lattice relaxation time, and f_k^{eq} is the equilibrium distribution function. The local equilibrium distribution function determines the type of problem that needs to be solved.

The equilibrium distribution functions are calculated with:

$$f_k^{\text{eq}} = \omega_k \rho \left[1 + \frac{\bar{c}_k \bar{u}}{c_s^2} + \frac{1}{2} \frac{(\bar{c}_k \bar{u})^2}{c_s^4} - \frac{1}{2} \frac{\bar{u} \bar{u}}{c_s^2} \right] \quad (2)$$

where ω_k is a weighting factor depending on the lattice Boltzmann model used, ρ – the lattice fluid density and

$$\omega_0 = \frac{4}{9}, \quad \omega_k = \frac{1}{9}, \quad k = 1, 2, 3, 4; \quad \omega_k = \frac{1}{36}, \quad k = 5, 6, 7, 8 \quad (3)$$

$$c_s = \frac{c_k}{\sqrt{3}}, \quad \bar{c}_k = \frac{\Delta x}{\Delta t} \hat{i} + \frac{\Delta y}{\Delta t} \hat{j}$$

To consider flow and temperature fields, the thermal LBM utilizes two distribution functions, f and g , for the flow and temperature fields, respectively. The f distribution function is as same as discussed above; the g distribution is as:

$$g_k(\bar{x} + \bar{c}_k \Delta t, t + \Delta t) = g_k(\bar{x}, t) + \frac{\Delta t}{\tau_g} \left[g_k^{\text{eq}}(\bar{x}, t) - g_k(\bar{x}, t) \right] \quad (4)$$

The corresponding equilibrium distribution functions are defined as [14, 22, 38]:

$$g_k^{\text{eq}} = \omega_k T \left[1 + \frac{\bar{c}_k \bar{u}}{c_s^2} \right] \quad (5)$$

Having computed the values of these local distribution functions, the flow properties are defined as:

$$\text{– flow density} \quad \rho = \sum_k f_k \quad (6)$$

$$\text{– momentum} \quad \rho u_i = \sum_k f_k \bar{c}_{ki} \quad (7)$$

$$\text{– temperature} \quad T = \sum_k g_k \quad (8)$$

where subscript i denotes the component of the Cartesian co-ordinates which implied summation for repeated indices. The Boussinesq approximation was applied and radiation heat transfer is neglected. In order to incorporate buoyancy force in the model, the force term in eq. (1) needs to be calculated as below in vertical direction (y):

$$\bar{F}_k = 3\omega_k g_y \beta \rho \theta \bar{c}_k \quad (9)$$

where β is the thermal expansion coefficient, \bar{c}_{ky} – the y -component of \bar{c}_k , ρ and θ are local density and dimensionless temperature, respectively. To simulate the natural convection problems with the LBM, it is necessary to determine the characteristic velocity $V = (\beta g_y \Delta T H)^{1/2}$ and then to obtain the corresponding kinetic viscosity (ν) and thermal diffusivity (α) through the following relationships involving the Prandtl number and Rayleigh number, respectively [15]:

$$\nu^2 = \frac{V^2 H^2 \text{Pr}}{\text{Ra}}, \quad \alpha = \frac{\nu}{\text{Pr}} \quad (10)$$

It implies that for different Rayleigh numbers both the kinetic viscosity (ν) and thermal diffusivity (α) cannot be fixed as constants in LBM simulations if the characteristic velocity (V) is kept constant (more information in [15]). The relaxation times, τ_v and τ_g , for flow and temperature lattice Boltzman equations given in eq. (1) and (4) can be determined by $\tau_v = \nu / c_s^2 \Delta t + 0.5$ and $\tau_g = \alpha / c_s^2 \Delta t + 0.5$

Entropy generation

Volumetric entropy generation due to heat transfer, S_T''' , and due to friction, S_P''' , are calculated as below:

$$S_T''' = \frac{k}{T^2} (|\Delta T|)^2, \quad S_P''' = \frac{\mu}{T} \varphi \quad (11)$$

where φ is defined by:

$$\varphi = \left(\frac{\partial u_i}{\partial x_j} + \frac{\partial u_j}{\partial x_i} \right) \frac{\partial u_i}{\partial x_j} \quad (12)$$

and the total volumetric entropy generation can be obtained by:

$$S_{gen}''' = S_T''' + S_P''' \quad (13)$$

The non-dimensional entropy generation rates, S_P^* , S_T^* , and S_{gen}^* in whole domain are defined by:

$$S_P^* = \frac{\int S_P''' dV}{\frac{\dot{Q}}{T_h}}, \quad S_T^* = \frac{\int S_T''' dV}{\frac{\dot{Q}}{T_h}}, \quad S_{gen}^* = \frac{\int S_{gen}''' dV}{\frac{\dot{Q}}{T_h}} \quad (14)$$

Boundary conditions

The distribution functions out of the domain are known from the streaming process. The unknown distribution functions are those toward the domain. Regarding the boundary conditions of the flow field, the solid walls are assumed to be no slip, and thus the bounce-back scheme is applied. This scheme specifies the outgoing directions of the distribution functions as the reverse of the incoming directions at the boundary sites. From the streaming process the distribution functions out of the domain are known. The unknown distribution functions are those toward the domain. In fig. 1 the unknown distribution function, which needs to be determined, are shown as dotted lines.

For example for flow field in the north boundary the following conditions is used

$$f_{4,n} = f_{2,n}, \quad f_{7,n} = f_{5,n}, \quad f_{8,n} = f_{6,n} \quad (15)$$

where n is the lattice on the boundary.

Furthermore, for the temperature field, the local temperature is defined as in eq. (8). The treatment of the temperature population (*i. e.* the distribution function g) at the adiabatic walls can be simplified by applying the bounce-back scheme to the temperature distribution function g_k such that a “heat flux-free state” is obtained in each lattice direction for the specific nodes associated with the adiabatic boundary condition. Applying this treatment for adiabatic walls yields (for bottom adiabatic boundary):

$$g_{3,n} = g_{3,n-1}, \quad g_{6,n} = g_{6,n-1}, \quad g_{7,n-1} = g_{7,n-1} \quad (16)$$

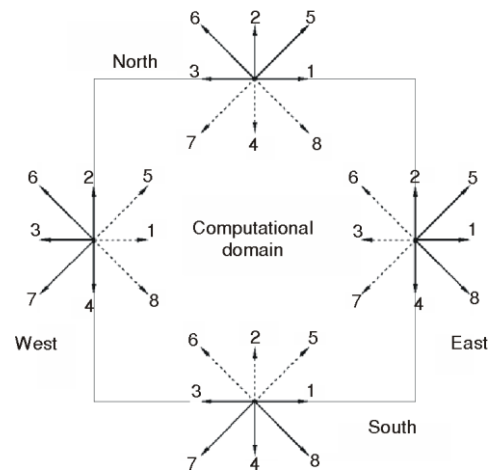


Figure 1. Domain boundaries and known (solid lines) and unknown (dotted lines) distribution functions

where n is the lattice on the boundary and $n - 1$ denotes the lattice inside the cavity adjacent to the boundary. For isothermal boundaries such as bottom hot wall the unknown distribution functions are evaluated as:

$$\begin{aligned} g_{2,n} &= T_h(\omega_2 + \omega_4) - g_{2,n} \\ g_{5,n} &= T_h(\omega_5 + \omega_7) - g_{7,n} \\ g_{6,n} &= T_h(\omega_6 + \omega_8) - g_{8,n} \end{aligned} \quad (17)$$

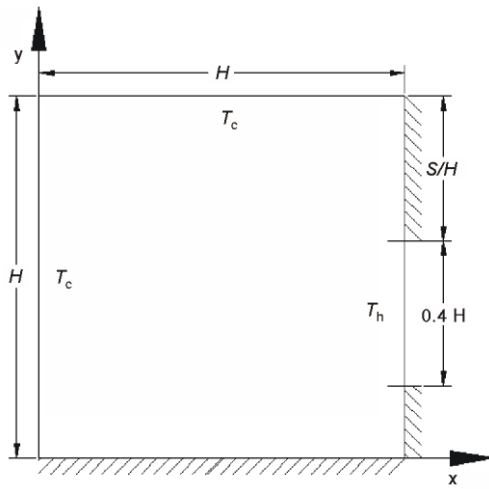


Figure 2. Schematic geometry of problem

Computational domain

The computational domain is a square cavity in which the left side and horizontal upper walls are isotherms. The heater (hot wall) is located at the right side wall of the cavity with length equal $0.4H$ and remained areas are adiabatic (fig. 2). The distance between heater and upper cold wall (S/H) changing from 0 to 0.6. In this study the Rayleigh number changes between 10^3 and 10^6 .

The Rayleigh number (Ra) and Nusselt number (Nu) for the current problem are defined as follows:

$$Ra = \frac{g_y \beta \Delta T H^3}{\alpha \nu} \quad (18)$$

Local Nusselt numbers are defined on isothermal walls in x- and y-directions as below:

$$\begin{aligned} Nu_x &= \frac{H}{T_h - T_c} \left. \frac{\partial T}{\partial x} \right|_{\text{wall}}, & \overline{Nu}_x &= \frac{1}{H} \int_0^H Nu_x dx \\ Nu_y &= \frac{H}{T_h - T_c} \left. \frac{\partial T}{\partial y} \right|_{\text{wall}}, & \overline{Nu}_y &= \frac{1}{H} \int_0^H Nu_y dy \end{aligned} \quad (19)$$

The numerical simulation was done by in house code which was written in FORTRAN using LBM. The written code was validated for the problem of natural convection within a 2-D square cavity [15, 39]. As mentioned before the simulations were based on the D2Q9 model. The Prandtl number was assumed to have a constant value of 0.71 in every case.

For validation and grid independency, the averaged Nusselt number was calculated at different Rayleigh numbers for different grid points. Table 1 shows the computed averaged Nusselt numbers in comparison with previous works (Kao *et al.* [15] and de Vahl [39]) for the grid point from 80×80 to 110×110 . It is due to the results presented at tab. 1; the grid point 100×100 was selected for all numerical simulations. Regarding to tab. 1, results show a good accuracy in comparison with previous studies.

Table 1. Comparison of averaged Nusselt numbers computed at different Rayleigh numbers using different grids with results presented in [15], and [39])

Ra		1,000	10,000	100,000	1,000,000
de Vahl Davis [39]		1.118	2.243	4.519	8.825
Kao <i>et al.</i> [15]		1.113	2.231	4.488	8.696
Present study	110 × 110	1.130	2.276	4.584	8.851
	100 × 100	1.131	2.278	4.578	8.833
	80 × 80	1.134	2.285	4.581	8.770

Results and discussion

In this study, the LBM has been used to investigate the effect of the heater location over the natural convection heat transfer and entropy generation. The fluid near the hot surface is warm and buoyancy effect causes to raise the fluid in cavity. The hot fluid carries heat to cold walls and moves to bottom of the cavity. This procedure repeats and creates a recirculation area. When the heater part moves to the cold wall ($S/H \rightarrow 0.0$), the hot fluid contacts to the cold wall immediately and becomes cold. This phenomenon causes to reduce the thermal diffusion in the cavity and subsequently the flow field and temperature gradient are dependent to the heater location intensively (fig. 3).

At low Rayleigh number, only one main recirculation region creates at the cavity which is independent from the heater location. While by increasing the Rayleigh number, a sensitive variation is observed in the flow field especially at the $S/H = 0.0$ (figs. 3 and 4). At high Rayleigh number, a small recirculation area is observed at the right side of the cavity when the heater is at $S/H = 0.0$ (fig. 3). At the low Rayleigh number, the dominant mechanism of heat transfer is conduction which is observed by the parallel isothermal lines (fig. 4).

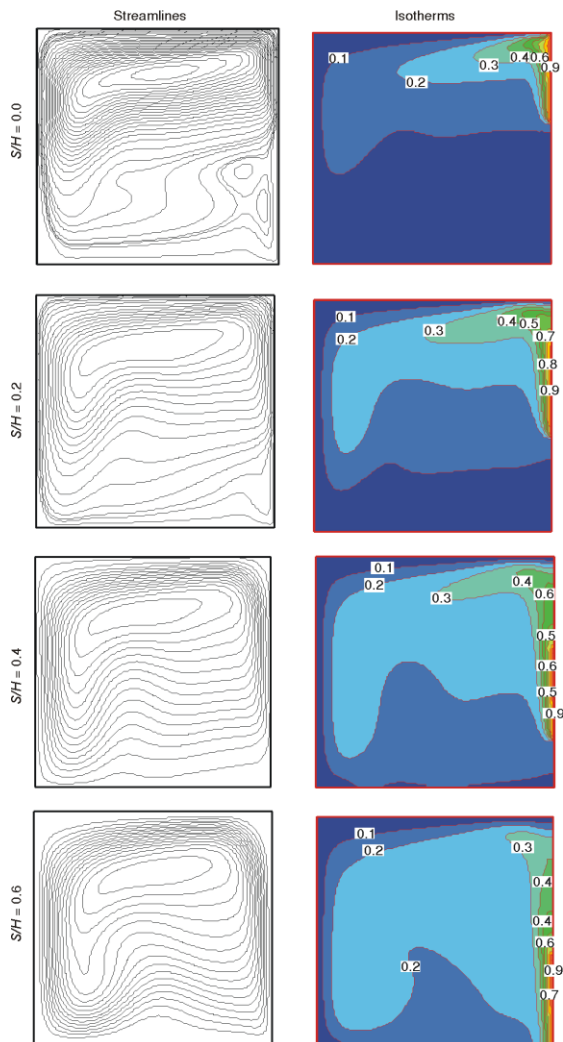


Figure 3. Streamlines and isotherm contours at $Ra = 10^6$ (color image see on our web site)

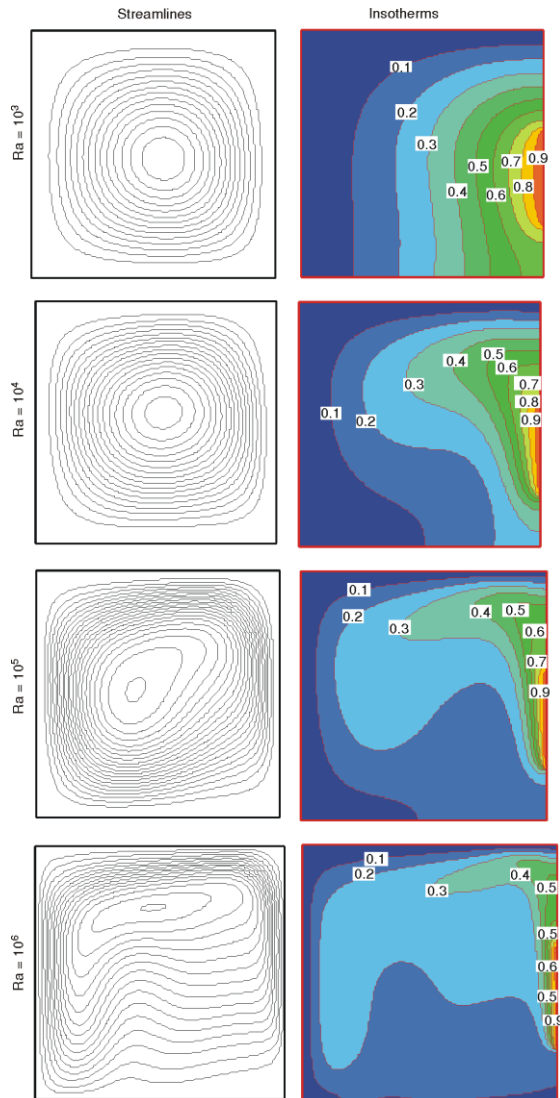


Figure 4. Streamlines and isotherm contours for $S/H = 0.4$ (color image see on our web site)

heater at different Rayleigh numbers is shown in fig. 6. When the heater goes toward to the cold wall (decreasing S/H) the temperature gradient increases so the dimensionless entropy generation increases. The distribution of the temperature contours is changed and subsequently the heat transfer from hot wall increases by increasing the Rayleigh number. This temperature contours causes to decrease the dimensionless entropy generation (see eq. 14). It can be seen that the maximum value of dimensionless entropy generation in all heater part location is achieved when Rayleigh number equals 10^4 .

On the other hand, by increasing the Rayleigh number the mechanism of the heat transfer conjugates between conduction and convection and finally the convection is dominant heat transfer mechanism at high Rayleigh number.

Variations of the flow and temperature fields affect the heat transfer parameters such as Nusselt number. The variations of the averaged Nusselt number over the different walls of the cavity at different Rayleigh numbers are shown in fig. 5. By decreasing the S/H , Nusselt number reduces which is due to the change of recirculation shape. On the other hand, the Nusselt number increases over the upper wall of the cavity at lower S/H . Accumulation of the several streamlines near the upper wall causes to increase the heat transfer from it. By increasing the distance between heater and cold wall, the heat transfer rate over the surface of the heater decreases. For the adjacency of heater and cold walls in the model with $S/H = 0.0$, the flow field has less effect on heat transfer rate from heater wall, so this model has less sensitively by increasing the Rayleigh number.

The value of entropy generation in flow field contains two parts: fluid friction and heat transfer. In laminar natural convection in cavity, the velocity gradient is small in comparison with temperature gradient so the entropy generation due to the friction is very small. The total dimensionless entropy generation for different positions of the

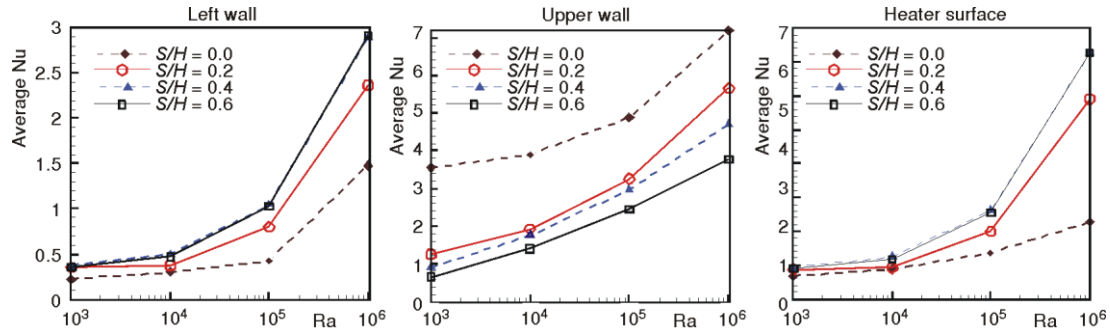


Figure 5. Variation of the averaged Nusselt number over the different walls for different S/H and Rayleigh numbers

According to the temperature contours, the mechanism of the heat transfer changes from conduction to the convection by increasing the Rayleigh number. This variation of heat transfer mechanism effects on the temperature gradient and subsequently increases the entropy generation. At Rayleigh number higher than 10^4 , the heat transfer rate increases more than the temperature gradient, so the entropy generation decreases. This is due to the dominant of the convection heat transfer in the cavity at high Rayleigh number.

Aghajani Delavar *et al.* [38] investigated the effect of the heater location on entropy generation, flow pattern, and heat transfer in a cavity which heater was located at the horizontal wall of the cavity. For better investigation, the results of [38] and this study were compared to gather in the following parts. The new averaged Nusselt number was defined by eq. 21 which is mean of the total Nusselt number over the cold walls and then the ratio of the present to previous studies [38] was computed:

$$Nu_{\text{average}} = \frac{\overline{Nu}_{\text{left}} + \overline{Nu}_{\text{up}}}{2} \quad (20)$$

$$Nu_{\text{ratio}} = \frac{\overline{Nu}_{\text{average-1}}}{\overline{Nu}_{\text{average-2}}} \quad (21)$$

In eq. 21, the index 1 and 2 turn on to the present study and results of [38], respectively. This ratio was also calculated for averaged Nusselt number over the heater part (fig. 7). Figure 7 shows that the heat transfer rate over the heater part is higher than when the heater was located over the horizontal wall at all Rayleigh numbers and heater locations. By increasing the Rayleigh number, the mechanism of heat transfer changes from the conduction

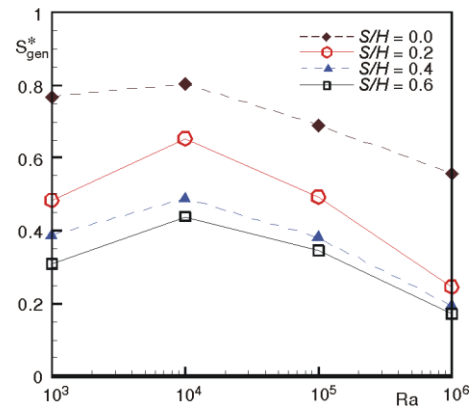


Figure 6. Non-dimensional volumetric entropy generation for different S/H at different Rayleigh numbers

to convection heat transfer. At $Ra = 10^3$, when the heater was located at the vertical wall, the dominant heat transfer mechanism is conduction. While for heater located at the horizontal wall, the heat transfer is affected by conduction and convection mechanisms. It should be mentioned that direction of the flow field is counter clockwise, so the heater surface is in direction of the cold fluid when is located at the horizontal wall. On the other hand, the hot flow must go longer distance to reach the cold walls of the cavity which causes to decrease the flow temperature and subsequently decreases the heat transfer from the cold walls. This phenomenon is unlike when the heater part is located at the vertical wall of the cavity. The averaged Nusselt number over the colds walls shows that the heat transfer increases when the heater part was located at the vertical wall except for $S/H = 0.2$ at Rayleigh number equal 10^4 . It is due to the transition of the heat transfer mechanism from the conduction to convection.

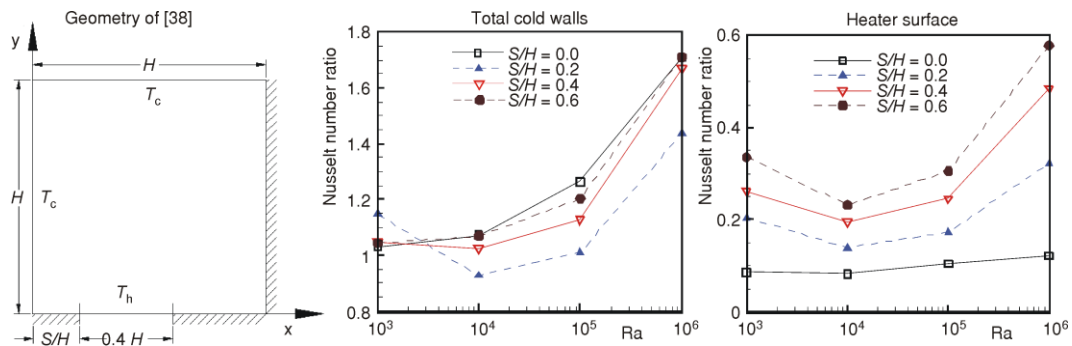


Figure 7. Ratio of the averaged total cold walls Nusselt number and heater surface Nusselt number vs. Rayleigh numbers for different S/H . The geometry of previous study[38] is in the left side

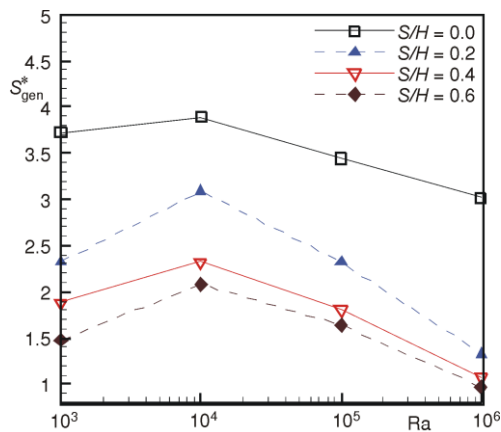


Figure 8. Ratio of non-dimensional volumetric entropy generation vs. Rayleigh number for different S/H

The dimensionless entropy generation ratio S_{gen}^* is shown in fig. 8 which was calculated by eq. 22. By increasing the temperature gradient in the cavity, the dimensionless entropy generation in the present study is more than the previous study which the heater was located at the horizontal wall. When the heater was located near the cold upper wall, the maximum temperature gradient exists in the cavity which causes to increase the entropy generation. By increasing the Rayleigh number, the convection heat transfer increases and subsequently the distribution of the temperature in the cavity is more monotony in comparison with low Rayleigh number. This variation in the temperature distribution causes to decrease the entropy generation. When the heater was located on the horizontal wall, this effect is more visible which is clear in fig. 8.

$$S_{\text{gen-ratio}}^* = \frac{S_{\text{gen-1}}^*}{S_{\text{gen-2}}^*} \quad (22)$$

Conclusions

In this study, the numerical simulation was done using 2-D thermal lattice Boltzmann method with the Boussinesq approximation. This study investigates the effect of changing the heater location on natural convection flows and entropy generation with non-linear phenomena within enclosed rectangular cavities. By increasing the S/H , Nusselt number rises for left and heater wall which is due to the amplifying the recirculation regions. The heater location has a main effect on the flow field and subsequently on temperature distribution in the cavity. The variation of the temperature contours shows its effect on the total dimensionless entropy generation in cavity. With increasing the Rayleigh number, the dimensionless entropy generation decreases at all heater positions. In comparison with authors pervious study it has been observed that the geometry in which the heater parts were located at side wall, were more sensitive to S/H .

The results show that heat transfer increases from the cold walls when the heater located on the vertical wall. The heat transfer rate increases from the heater surface when the heater located on the horizontal wall of the cavity.

Nomenclature

\bar{c}_k	– discrete lattice velocity in direction k
\bar{F}_k	– external force in direction of lattice velocity
f_k^{eq}	– equilibrium distribution
H	– duct width, [m]
k	– thermal conductivity, [$\text{Wm}^{-1}\text{K}^{-1}$]
Nu	– local Nusselt number, ($= hx/k_f$), [–]
Pr	– Prandtl number, ($= \nu/\theta$), [–]
Q	– heat transfer, [W]
Ra	– Rayleigh number, ($= g_y \beta \Delta TH^3 / \alpha \nu$), [–]
S_{gen}^m	– total volumetric entropy generation rate, [$\text{Wm}^{-3}\text{K}^{-1}$]
S_p^m	– volumetric entropy generation rate due to friction, [$\text{Wm}^{-3}\text{K}^{-1}$]
S_T^m	– volumetric entropy generation rate due to heat transfer, [$\text{Wm}^{-3}\text{K}^{-1}$]
T_c	– cold temperature, [K]
T_h	– hot temperature, [K]
Δt	– lattice time step
u, v	– horizontal and vertical components of the velocity, [ms^{-1}]
V	– characteristic velocity of natural convection ($= \beta g_y \Delta TH$) ^{1/2} , [ms^{-1}]

Greek symbols

α	– thermal diffusivity, [m^2s^{-1}]
β	– thermal expansion coefficient, [K^{-1}]
θ	– dimensionless temperature, ($T - T_c / T_h - T_c$)
μ	– molecular viscosity, [$\text{kgm}^{-1}\text{s}^{-1}$]
ν	– kinetic viscosity, [m^2s^{-1}]
ρ	– density, [kgm^{-3}]
τ	– lattice relaxation time
ω_k	– weighting factor

Subscripts

c	– cold
gen	– total generated
h	– hot
T	– due to heat transfer
P	– due to friction
k	– streaming direction
i	– i-direction
y	– y-direction

Superscript

eq	– equilibrium
----	---------------

Acronym

LBM	– lattice Boltzman method
-----	---------------------------

Reference

- [1] Chu, H. H., Churchill, S. W., The Effect of Heater Size, Location, Aspect-Ratio and Boundary Conditions on Two-Dimensional Laminar Natural Convection in Rectangular Channels, *Journal of Heat Transfer*, 98 (1976), 2, pp. 194-201

- [2] Refai, A. G., Yovanovich, M. M., Influence of Discrete Heat Source Location on Natural Convection Heat Transfer in a Vertical Square Enclosure, *Journal of Electronic Packaging September*, 113 (1991), 3, pp. 268-274
- [3] Refai, A. G., Yovanovich, M. M., Numerical Study of Natural Convection from Discrete Heat Sources in a Vertical Square Enclosure, *Journal of Thermophysics and Heat Transfer*, 6 (1992), 1, pp. 121-127; AIAA paper No. 90-0256, Originally presented at AIAA 28th Aerospace Sciences Meeting, Reno, Nev., USA, 1990
- [4] Nelson, J. E. B., Balakrishnan, A. R., Murthy, S. S., Experiments on Stratified Chilledwater Tanks, *Int. J. Refrig.* 22 (1999), 3, pp. 216-234
- [5] Ampofo, F., Karayiannis, T. G., Experimental Benchmark Data for Turbulent Natural Convection in an Air Filled Square Cavity, *Int. J. Heat Mass Transfer*, 46 (2003), 19, pp. 3551-3572
- [6] Adeyinka, O. B., Naterer, G. F., Experimental Uncertainty of Measured Entropy Production with Pulsed Laser PIV and Planar Laser Induced Fluorescence, *Int. J. Heat Mass Transfer*, 48 (2005), 8, pp. 1450-1461
- [7] Poujol, F.T., Natural Convection of a High Prandtl Number Fluid in Cavity, *Int. Comm. Heat Mass Transfer*, 27 (2000), 1, pp. 109-118
- [8] Oliveski, R. D. C., Krenzinger, A., Vielmo, H. A., Cooling of Cylindrical Vertical Tank Submitted to Natural Internal Convection, *Int. J. Heat Mass Transfer*, 46 (2003), 11, pp. 2015-2026
- [9] Basak, T., Roy, S., Balakrishnan, A. R., Effects of Thermal Boundary Conditions on Natural Convection Flows within a Square Cavity, *Int. J. Heat Mass Transfer*, 49 (2006), 23-24, pp. 4525-4535
- [10] Basak, T., Aravind, G., Roy, S., Visualization of Heat Flow Due to Natural Convection within Triangular Cavities Using Bejan's Heatline Concept, *Int. J. Heat Mass Transfer*, 52 (2009), 11-12, pp. 2824-2833
- [11] Beya, B. B., Lili, T., Transient Natural Convection in 3-D Tilted Enclosure Heated from Two Opposite Sides, *Int. Comm. Heat Mass Transfer*, 36 (2009), 6, pp. 604-613
- [12] Chen, S., Doolen, G. D., Lattice Boltzmann Method for Fluid Flows, *Annu. Rev. Fluid Mech.*, 30 (1998), pp. 329-364
- [13] Succi, S., *The Lattice Boltzmann Equation for Fluid Dynamics and Beyond*, Clarendon Press, Oxford, UK, 2001
- [14] Mohammad, A. A., *Applied Lattice Boltzmann Method for Transport Phenomena, Momentum Heat and Mass Transfer*, The University of Calgary Press, Calgary, Alb., Canada, 2007
- [15] Kao, P. H., Chen, Y. H., Yang, R. J., Simulations of the Macroscopic and Mesoscopic Natural Convection Flows within Rectangular Cavities, *Int. J. of Heat Mass Transfer*, 51 (2008), 15-16, pp. 3776-3793
- [16] Chopard, B., Luthi, P. O., Lattice Boltzmann Computations and Applications to Physics, *Theor. Comput. Phys.*, 217 (1999), 1, pp. 115-130
- [17] Nourgaliev, R. R., *et al.*, The Lattice Boltzmann Equation Method: Theoretical Interpretation, Numerics and Implications, *Int. J. Multiphase Flow*, 29 (2003), 1, pp. 117-169
- [18] He, X., Chen, S., Doolen, G. D., A Novel Thermal Model for the Lattice Boltzmann Method in Incompressible Limit, *J. Comput. Phys.*, 146 (1998), 1, pp. 282-300
- [19] Barrios, G., *et al.*, The Lattice Boltzmann Equation for Natural Convection in a Two-Dimensional Cavity with a Partially Heated Wall, *J. Fluid Mech.*, 522 (2005), pp. 91-100
- [20] Dixit, H. N., Babu, V., Simulations of High Rayleigh Number Natural Convection in a Square Cavity Using the Lattice Boltzmann Method, *Int. J. Heat Mass Transfer*, 49 (2006), 3-4, pp. 727-739
- [21] D'Orazio, A., Corcione, M., Celata, G. P., Application to Natural Convection Enclosed Flows of a Lattice Boltzmann BGK Model Coupled with a General Purpose Thermal Boundary Condition, *Int. J. Thermal Sciences*, 43 (2004), 6, pp. 575-586
- [22] Mezrhab, A., *et al.*, Lattice-Boltzmann Modelling of Natural Convection in an Inclined Square Enclosure with Partitions Attached to its Cold Wall, *Int. J. Heat and Fluid Flow*, 27 (2006), 3, pp. 456-465
- [23] Jami, P., Mezrhab, A., Bouzidi, M., Lallemand, Lattice Boltzmann Method Applied to the Laminar Natural Convection in an Enclosure with a Heat-Generating Cylinder Conducting Body, *Int. J. Thermal Sciences*, 46 (2007), 1, pp. 38-47
- [24] Mohamad, A. A., El-Ganaoui, M., Bennacer, R., Lattice Boltzmann Simulation of Natural Convection in an Open Ended Cavity, *Int. J. Thermal Sciences*, 48 (2009), 10, pp. 1870-1875
- [25] Peng, Y., Shu, C., Chew, Y. T., A 3-D Incompressible Thermal Lattice Boltzmann Model and Its Application to Simulate Natural Convection in a Cubic Cavity, *Journal of Computational Physics*, 193 (2003) 1, pp. 260-274

- [26] Bejan, A., *Entropy Generation through Heat and Fluid Flow*, John Wiley and Sons, New York, USA, 1982
- [27] Bejan, A., *Entropy Generation Minimization*, CRC Press, Boca Raton, Fla., USA, 1996
- [28] Bejan, A., *Advanced Engineering Thermodynamics*, 2nd ed., John Wiley and Sons, New York, USA, 1997
- [29] Bejan, A., Second-Law Analysis in Heat Transfer, *Energy*, 5 (1980), 8-9, pp. 720-732
- [30] Bejan, A., Second-Law Analysis in Heat Transfer and Thermal Design, *Adv. Heat Transfer*, 15 (1982), pp. 1-58
- [31] Bejan, A., Fundamentals of Exergy Analysis, Entropy-Generation Minimization, and the Generation of Flow Architecture, *Int. J. Energy Research*, 26 (2002), 7, pp. 545-65
- [32] Demirel, Y., Kahraman, R., Thermodynamic Analysis of Convective Heat Transfer in an Annular Packed Duct, *Int. J. Heat and Fluid Flow*, 21 (2000), 4, pp. 442-448
- [33] Sahin, A. Z., A Second-Law Comparison for Optimum Shape of Duct Subjected to Constant Wall Temperature and Laminar Flow, *J. Heat Mass Transfer*, 33 (1998), 5-6, pp. 425-430
- [34] Narusawa, U., The Second-Law Analysis of Mixed Convection in Rectangular Ducts, *J. Heat Mass Transfer*, 37 (2001), 2-3, pp. 197-203
- [35] Mahmud, S., Fraser, R. A., Thermodynamic Analysis of Flow and Heat Transfer Inside a Channel with Two Parallel Plates, *Exergy*, 2 (2002), 2, pp. 140-146
- [36] Mahmud, S., Fraser, R. A., The Second-Law Analysis in Fundamental Convective Heat-Transfer Problems, *Int. J. Therm. Sci.*, 42 (2003), 2, pp. 177-186
- [37] Aïboud-Saouli, S., *et al.*, Second-Law Analysis of Laminar Fluid Flow in a Heated Channel with Hydromagnetic and Viscous Dissipation Effects, *Applied Energy*, 84 (2007), 3, pp. 279-289
- [38] Delavar, M. A., Farhadi, M., Sedighi, K., Effect of the Heater Location on Heat Transfer and Entropy Generation in the Cavity Using the Lattice Boltzmann Method, *Heat Transfer Research*, 40 (2009), 6, pp. 521-536
- [39] Vahl Davis, G. D., Natural Convection of Air in a Square Cavity: a Bench Mark Numerical Solution, *Int. J. Numer. Methods Fluids*, 3 (1983), 3, pp. 249-264